

1 **Supplementary Material**

2 **SI Materials and Methods**

3 The pyrene fluorescence loss method is a novel approach to quantify a broader portion of
4 the BC combustion continuum (Flores-Cervantes et al., 2009). BC concentrations were
5 calculated from the loss of dissolved pyrene based on eq. 1 – 3.

$$6 \quad f_w = \frac{C_f}{C_i} \quad (\text{eq. 1})$$

7 Where f_w is the fraction of pyrene lost from solution due to adsorption to the BC, i.e. ratio
8 of the final (C_f) to the initial pyrene concentration (C_i).

$$9 \quad K_d = \frac{(1-f_w)}{f_w r_{sw}} \quad (\text{eq. 2})$$

10 The solid-water partitioning coefficient (K_d) for pyrene was determined using eq. 2, where
11 r_{sw} is the solid-water ratio (kg L^{-1}).

$$12 \quad f_{BC} = \frac{[K_d - f_{OC} K_{OC}]}{K_{BC} C_w^{n-1}} \quad (\text{eq. 3})$$

13 The calculated K_d was used to determine the fraction of BC (f_{BC}) according to eq. 3. The K_{OC}
14 and K_{BC} are the previously determined pyrene partitioning coefficients of $10^{4.7}$ (L kgOC^{-1})
15 for organic carbon (OC) and $10^{6.25}$ (L kgBC^{-1}) for BC (BC), respectively (Accardi-Dey and
16 Gschwend, 2002). The C_w^{n-1} is the initial truly dissolved pyrene concentration, where n is
17 the Freundlich exponent of 0.62. An initial concentration of $1 \mu\text{g L}^{-1}$ pyrene was purposely
18 selected to allow the C_w term to approach 1 since the Freundlich exponent is the

19 component with the highest degree of uncertainty. Finally, the f_{OC} is the fraction of the
20 total organic carbon determined by the IRMS during the CTO-375 analysis. We assumed
21 that BC would be a minor constituent so that the total organic carbon would be equivalent
22 to the organic carbon concentration, as was done in Flores-Cervantes (2009).

23

24 Additionally, the salinity of five pyrene solutions with double the filter mass and half the
25 volume were measured with a refractometer in order to assess if salinity could have
26 affected pyrene's solubility in solution. A measurement of 0 ppt was received in triplicate
27 for all five samples, concluding that the salting out effect of pyrene would be minimal in
28 our set-up.

29

30 A series of blank filters were placed on a high volume air sampler at the Graduate School
31 of Oceanography, Narragansett, Rhode Island at a rate of $1.35 \text{ m}^3 \text{ min}^{-1}$ (47.5 CFM) for 10,
32 20, 30, 60, and 120 minutes to test if the carbon blank would decrease inversely as air
33 volume filtered increased. The associated carbon blank was constant for all air volumes,
34 suggesting that the carbon detected by the thermal methods was not due to
35 contamination but rather the filter matrix.

36

37 In separate work, corn pollen was analyzed by both CTO-375 and the pyrene fluorescence
38 loss technique to assess its possible interference on the BC measurements. No BC was

39 detected on the pollen using the pyrene fluorescence loss method; however
40 approximately 66% of the pollen remained after the CTO-375 treatment.

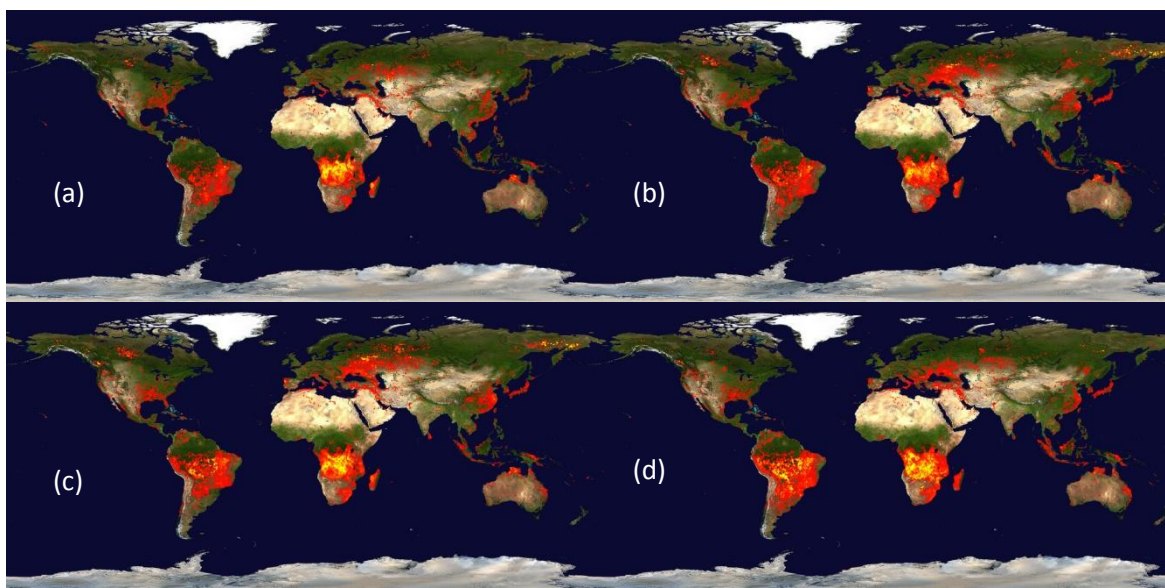
41

42 Methodological quality control for the CTO-375 and pyrene fluorescence loss method was
43 also assessed and compared using the NIST standard reference materials 1941b (marine
44 sediment). BC mass fractions for were within the expected range of $0.7 \pm 0.1\%$ for the
45 CTO-375 method and 1.6% for the pyrene fluorescence loss (Hammes et al., 2007; Flores-
46 Cervantes et al., 2009).

47

48 **SI Tables and Figures**

49



50

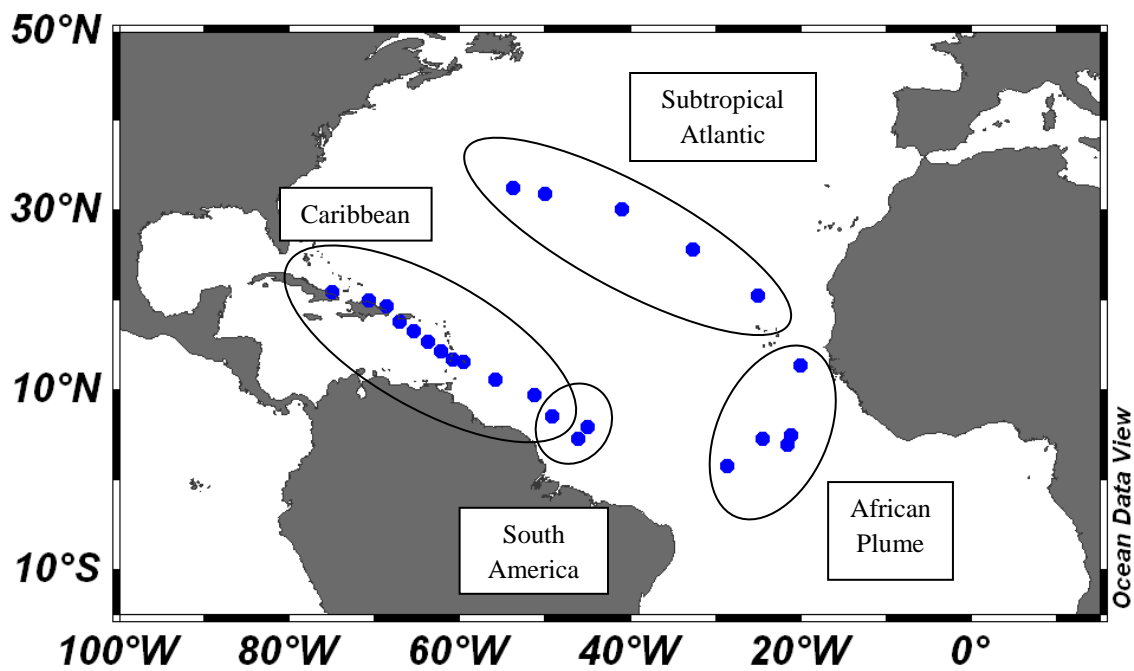
51

52

53 **SI Fig. 1.** Global fire maps generated from the MODIS Terra and Aqua satellites for (a) June
54 30-July 9 2010, (b) July 20-27, 2010, (c) July 30-August 8, 2010, and (d) August 18-28,

55 2010. Both (a) and (b) co-occurred during the Caribbean and South America region
56 sampling, (c) occurred during the African plume region sampling, and (d) for the
57 subtropical Atlantic region sampling. The color indicates the number of detected wildfires
58 from red (low) to yellow (high). Credits: Jacques Descloitres, Louis Giglio, and Reto Stokli.

59



60

61 **SI Fig. 2.** Filter samples grouped by region, as defined by wind direction and locality to
62 land. Note that the Amazon and African Plume regions were below the inter-tropical
63 convergence zone at the time of sampling.

64

65

66

67

68

69

70

Sample	Start Date (2010)	Minutes Sampled	Latitude	Longitude	Volume (m³)
QFF-1	6-Jul	721.2	20.983	-74.988	408
QFF-2	7-Jul	725.4	20.021	-70.654	308
QFF-3	7-Jul	684.0	19.285	-68.575	97
QFF-4	8-Jul	736.6	17.615	-67.033	104
QFF-5	8-Jul	707.3	16.550	-65.483	100
QFF-6	9-Jul	740.6	15.416	-63.783	315
QFF-7	9-Jul	708.4	14.338	-62.223	301
QFF-8	10-Jul	691.2	13.453	-60.817	294
QFF-9	14-Jul	2822.6	7.079	-49.156	1199
QFF-10	16-Jul	2455.0	5.906	-45.011	1043
QFF-11	20-Jul	2884.1	11.179	-55.835	1225
QFF-12	22-Jul	1419.6	13.100	-59.650	603
QFF-13	23-Jul	2793.7	9.483	-51.266	3758
QFF-14	27-Jul	3286.7	4.600	-46.200	4421
QFF-15	30-Jul	3983.4	1.580	-28.767	5358
QFF-16	3-Aug	3353.1	3.961	-21.667	4510
QFF-17	6-Aug	4532.0	4.977	-21.215	6096
QFF-18	10-Aug	2234.8	4.554	-24.496	3006
QFF-19	15-Aug	2209.0	12.813	-20.066	2971
QFF-20	21-Aug	2682.2	20.521	-25.118	3608
QFF-21	23-Aug	2718.1	25.717	-32.768	3656
QFF-22	25-Aug	2863.3	30.167	-41.027	3851
QFF-23	27-Aug	2846.1	31.871	-50.100	3828
QFF-24	29-Aug	943.2	32.516	-53.764	1269

71

72 SI Table 1. Date, location, and volume of air sampled for each filter.

73

74

75

76

77

78

79

QFF	CTO-375	PFL	TOT	OT-21	Region
1	0.00	0.62	0.32	0.00	Caribbean
2	1.17	1.12	0.00	0.08	Caribbean
3	0.64	3.56	0.00	0.52	Caribbean
4	3.37	2.86	0.00	0.72	Caribbean
5	1.71	2.98	0.00	0.00	Caribbean
6	1.02	0.95	0.00	0.16	Caribbean
7	0.00	0.99	0.00	0.08	Caribbean
8	1.39	0.00	0.00	0.00	Caribbean
9	0.02	0.19	0.00	0.14	Caribbean/South America
10	0.35	0.42	0.00	0.53	South America
11	0.04	0.06	0.00	0.18	Caribbean
12	0.83	0.53	0.00	0.14	Caribbean
13	0.02	0.25	0.00	0.23	Caribbean
14	0.09	0.33	0.06	0.19	South America
15	0.04	0.33	0.00	0.20	African Plume
16	0.01	0.47	0.03	0.83	African Plume
17	0.08	0.21	0.03	0.92	African Plume
18	0.03	0.91	0.03	1.33	African Plume
19	0.19	0.74	0.01	0.73	African Plume
20	0.03	0.36	0.00	0.30	Subtropical Atlantic
21	0.02	0.40	0.00	0.33	Subtropical Atlantic
22	0.03	0.00	0.18	0.09	Subtropical Atlantic
23	0.03	0.09	0.00	0.13	Subtropical Atlantic
24	0.30	0.56	0.14	0.00	Subtropical Atlantic

80

81 SI Table 2: Black carbon concentration ($\mu\text{g m}^{-3}$) per individual filter for each method.

82

83

84

85

86

87

88

Sample	TOC ^a ug m ⁻³	TOC ^b ug m-3	δ ¹³ C-TOC	δ ¹³ C-BC
1	0.4	0.9	-22	2
2	2.1	2.3	-32	-91
3	3.1	3.9	-27	-64
4	3.8	6.1	-27	-39
5	5.8	5.2	-34	-41
6	1.1	0.4	-33	-42
7	1.2	0.8	-9	-17
8	1.9	1.6	-26	-36
9	0.4	0.4	-24	-16
10	0.5	0.9	-26	-35
11	1.0	0.4	22	-23
12	0.8	0.7	-28	-40
13	0.3	0.4	-27	-6
14	0.2	0.2	-32	-34
15	0.1	0.2	-26	-18
16	0.7	1.1	-19	-26
17	1.3	1.6	-19	-16
18	1.5	1.9	-20	-2
19	0.7	0.9	-22	-24
20	0.2	0.4	-23	-13
21	0.3	0.4	-24	3
22	0.2	0.1	-25	-27
23	0.2	0.2	-17	-17
24	0.2	0.4	-25	-21

89

90 SI Table 3: Total organic carbon concentrations as measured by the CTO-375 (TOC^a) and
91 TOT (TOC^b) methods and the δ¹³C values for the total organic carbon and black carbon
92 determined for each filter by the CTO-375 method after blank correction.

93

94

95

96

97

98

99

Regional Average	CTO/PFL	BC/TOC-IRMS	BC/TOC-TOT
Caribbean	1.2	0.45	0.16
South America	0.6	0.45	0.40
African Plume	0.3	0.13	0.73
Subtropical Atlantic	0.2	0.36	0.67
1650 diesel particulate matter	3.1	0.62	

100

101 SI Table 4: Regional average of soot-like black carbon (CTO-375) to the broader black
102 carbon spectrum (PFL) ratio and the ratio of black carbon in the total organic carbon
103 determined by the CTO-375 method and TOT.

104

105 **SI References**

106

107 Accardi-Dey, A., and Gschwend, P. M.: Assessing the combined roles of natural organic
108 matter and black carbon as sorbents in sediments, *Environ Sci Technol*, 36, 21-29, Doi
109 10.1021/Es010953c, 2002.

110 Flores-Cervantes, D. X., Reddy, C. M., and Gschwend, P. M.: Inferring Black Carbon
111 Concentrations in Particulate Organic Matter by Observing Pyrene Fluorescence Losses,
112 *Environ Sci Technol*, 43, 4864-4870, Doi 10.1021/Es900043c, 2009.

113 Hammes, K., Schmidt, M. W. I., Smernik, R. J., Currie, L. A., Ball, W. P., Nguyen, T. H.,
114 Louchouart, P., Houel, S., Gustafsson, O., Elmquist, M., Cornelissen, G., Skjemstad, J. O.,
115 Masiello, C. A., Song, J., Peng, P., Mitra, S., Dunn, J. C., Hatcher, P. G., Hockaday, W. C.,
116 Smith, D. M., Hartkopf-Froeder, C., Boehmer, A., Luer, B., Huebert, B. J., Amelung, W.,
117 Brodowski, S., Huang, L., Zhang, W., Gschwend, P. M., Flores-Cervantes, D. X., Largeau, C.,
118 Rouzaud, J. N., Rumpel, C., Guggenberger, G., Kaiser, K., Rodionov, A., Gonzalez-Vila, F. J.,
119 Gonzalez-Perez, J. A., de la Rosa, J. M., Manning, D. A. C., Lopez-Capel, E., and Ding, L.:
120 Comparison of quantification methods to measure fire-derived (black/elemental) carbon
121 in soils and sediments using reference materials from soil, water, sediment and the
122 atmosphere, *Global Biogeochem Cy*, 21, Artn Gb3016 Doi 10.1029/2006gb002914, 2007.